~~Conference~~

Chemical studies of elements with $Z \geq 104$ in liquid phase

Yuichiro Nagame[a*], Jens Volker Kratz[b], Matthias Schädel[a]

[a]*Advanced Science Research Center, Japan Atomic Energy Agency (JAEA), Tokai, Ibaraki 319-1195, Japan*
[b]*Institut für Kernchemie, Johannes Gutenberg-Universität Mainz, Fritz-Straßmann-Weg 2, 55128 Mainz, Germany*

Abstract

Recent studies of the chemical separation and characterization experiments of the first three transactinide elements, rutherfordium (Rf), dubnium (Db), and seaborgium (Sg), conducted atom-at-a-time in liquid phases, are reviewed. A short description on experimental techniques based on partition methods, specifically automated rapid chemical separation systems, is also given. A newly developed experimental approach to investigate single atoms of the heaviest elements with an electrochemical method is introduced. Perspectives for liquid-phase chemistry experiments on heavier elements are briefly discussed.

Keywords: Atom-at-a-time (single-atom) chemistry; Transactinide elements; Rapid chemical separations; Ion-exchange chromatography; Reversed-phase extraction chromatography; Liquid-liquid extraction; Flow electrolytic column chromatography

1. Introduction

Chemical studies of the heaviest elements at the farthest reach of the Periodic Table are extremely fascinating and challenging not only in nuclear and radiochemistry but also general chemistry [1-5]. Very important and interesting aspects are to clarify basic chemical properties of these elements, such as ionic radii, redox potentials, or their ability to form chemical compounds as well as to elucidate the influence of relativistic effects on valence electrons of heavy elements and the impact on chemical properties of these elements [6-8]. The transactinides are elements with atomic numbers $Z \geq 104$. They are all man-made elements synthesized at accelerators using nuclear reactions of heavy-ion beams with heavy element target materials and they can only be identified by measuring their characteristic nuclear decay or that of their known daughter nuclei with sensitive detection techniques. As both half-lives and cross sections of these nuclides are rapidly decreasing, they are usually available in quantities of only a few atoms or often one atom at a time.

The chemical characterization of transactinide elements in liquid-phase experiments has been accomplished by partition methods with single atoms, e.g., liquid-liquid extraction, ion-exchange chromatography, and reversed-phase extraction chromatography. The ultimate goal of these atom-at-a-time scale partition experiments is to determine the so-called distribution coefficient, K_d, as a function of ligand concentration. The K_d value is given in its simplest definition as the ratio of the number of atoms - determined by its radioactivity - either in the organic phase (in liquid-liquid extractions) or in the

* Corresponding author. Tel.: +81-29-282-5416; fax: +81-29-282-5927.
E-mail address: nagame.yuichiro@jaea.go.jp.

stationary phase (in column chromatography) to that in the aqueous liquid phase. In order to get statistically significant results, it is indispensable to repeat the same experimental procedure several hundred or even several thousand times with cycle times of about the lifetime of the nuclide under investigation. In these processes, the behavior of the transactinide element is compared with that of its lighter homologs under identical conditions. Recent investigations have been carried out with automated rapid chemical separation apparatuses to characterize chemical properties of these elements.

Firstly, we mention the concept of single-atom chemistry from the view point of kinetic and thermodynamic aspects. Then, we summarize recent studies of the chemical separation and characterization experiments of the three transactinide elements so far investigated in liquid phases, rutherfordium (Rf), dubnium (Db), and seaborgium (Sg), report about the chemical properties that were obtained, and give some perspectives for further studies. A new experimental approach, electrochemistry, to the heaviest elements with single atoms is briefly introduced. Large parts of this paper are based on modifications of the previous review articles [9-11]. The more comprehensive reviews on recent chemical investigations of the transactinide elements are published in [1-5].

2. Single-atom chemistry

A comment is in order on the special situation in which chemistry has to be studied with single atoms. For a chemical reaction

$$a\mathrm{A} + e\mathrm{E} \rightleftarrows x\mathrm{X} + z\mathrm{Z}, \tag{1}$$

the change of the Gibbs free energy is

$$\Delta G = \Delta G_0 + RT \frac{[\mathrm{X}]^x\,[\mathrm{Z}]^z}{[\mathrm{A}]^a\,[\mathrm{E}]^e}, \tag{2}$$

where the brackets indicate activities (concentrations) of the substances involved. According to the ‘law of mass action’,

$$\frac{[\mathrm{X}]^x\,[\mathrm{Z}]^z}{[\mathrm{A}]^a\,[\mathrm{E}]^e} = K \tag{3}$$

where K is the equilibrium constant. In equilibrium, $\Delta G = 0$, and

$$\Delta G_0 = -RT \ln K\,. \tag{4}$$

This is well established for macroscopic quantities where, e.g., ions of the metal M are constituents of A and X at the same time. Eq. (1) characterizes a dynamical and reversible process in which reactants and products are continuously transformed into each other back and forth even at equilibrium. If only one atom of M is present, however, it cannot be a constituent of A and X at the same time, and at least one of the activities on the left or right hand side of Eq. (1) is zero. Consequently, an equilibrium constant can no

longer be defined, and the same holds for the thermodynamic function ΔG_0. Does it make sense, then, to study chemical equilibria with a single atom?

Guillaumont et al. [12, 13], in view of this dilemma, pointed out that chemical speciation of nuclides at the tracer scale is usually feasible with partition methods in which the species to be characterized is distributed between two phases. This can be an aqueous and an organic phase or a solid phase and the gas phase. According to Guillaumont et al. [12], single-atom chemistry requires the introduction of a specific thermodynamic function, the single-particle Gibbs free energy. An expression equivalent to the law of mass action is derived by Guillaumont et al. [12] in which activities (concentrations) are replaced by the probability of finding the species in the appropriate phase. According to this law, an equilibrium constant, i.e., the distribution coefficient K_d of M between two phases, is correctly defined in terms of the probabilities of finding M in one phase or the other. If a static partition method is used, this coefficient must be measured many times in repetitive experiments. Since dynamical partition methods (chromatographic separations) can be considered as spatially repetitive static partitions, the displacement of M along the chromatographic column, in itself, is a statistical result and only one experiment is necessary, in principle. This underlines the validity of partition experiments with single atoms and the particular attractivity of chromatographic methods in single-atom chemistry.

For short-lived atoms, additional considerations with regard to the kinetics of the reaction are in order. The partition equilibrium must be reached during the short lifetime of the atom which requires high reaction rates. Let us consider a single-step exchange reaction

$$\mathrm{MX + Y} \underset{k_2}{\overset{k_1}{\rightleftarrows}} \mathrm{MY + X.} \tag{5}$$

Here, M is the single atom that can bind with either X or Y, and k_1 and k_2 are the rate constants for the reactions forth and back, respectively. The rate of a chemical reaction depends on the height of the reaction barrier between the states MX + Y and MY + X, because in-between, there is a state of high potential energy (the transition state [Y...M...X]). This state is unstable because the old chemical bond is not completely disrupted and the new one not yet completely formed. If the (Gibbs free) energies of activation $\Delta G^{\#}_1$ and $\Delta G^{\#}_2$ are high, the reaction proceeds very slowly, where $\Delta G^{\#}_1$ and $\Delta G^{\#}_2$ indicate the energy differences between the initial state (reactants: MX + Y) and the transition state [Y...M...X] and the final state (products: MY + X) and [Y...M...X]. The transitions from left to right and from right to left do not occur with sufficient frequency and the system is far from its thermodynamical equilibrium. Borg and Dienes [14] found that only if $\Delta G^{\#}$ (the mean values of $\Delta G^{\#}_1$ and $\Delta G^{\#}_2$) is less than 15 kcal (60 kJ), then the residence time of M in either state (MX or MY) is rather short (< 1 s) and an equilibrium is rapidly reached (in comparison with the nuclear half-lives of the transactinide nuclides). They further pointed out that the average time that M spends as MX or MY is proportional to the equilibrium constant. Thus, a measurement of the partition of M between the states MX and MY with very few atoms of M will already yield an equilibrium constant close to the 'true' value provided that both states are rapidly sampled. This shows again that chromatographic systems with fast kinetics are ideally suited for single-atom separations as there is rapid and multiple sampling of the absorbed or mobile species. The fractional average time that M spends as the absorbed species (which is proportional to the equilibrium constant) is closely related to the chromatographic observable, the retention time; see also [15] for further discussion of kinetic and thermodynamic aspects of single-atom chemistry.

3. Liquid-phase experiments

3.1. First survey experiments

According to the actinide concept by Seaborg [16], the 5f-electron series in the Periodic Table ends with element 103, lawrencium (Lr), and a new 6d-electron transition series starts with $Z = 104$, Rf. After discovery of a long-lived α-particle emitting isotope with a half-life of 68 s, ^{261}Rf, by Ghiorso et al. [17], Silva et al. confirmed the placement of Rf as the first transactinide element into group 4 of the Periodic Table by conducting the first liquid phase separations with a cation-exchange chromatography column and the chelating agent α-hydroxyisobutyric acid (α-HiB) [18]. In this pioneering experiment, ^{261}Rf was produced in an irradiation of 47 µg of ^{248}Cm electrodeposited over 0.2 mm^2 area onto a beryllium (Be) foil, with 92-MeV ^{18}O ions delivered by the Berkeley Heavy Ion Linear Accelerator (HILAC). The experiment, even though being "historical", was typical for many liquid phase experiments performed later. It combined a fast transport system for transfer of reaction products from a target-recoil chamber to a chemistry system with a discontinuously performed chemical separation that is typically repeated hundreds/thousands of times. It also included the preparation of sources for α-particle spectroscopy by rapid evaporation of the aqueous effluent from the column to dryness and recorded energy and time of α events and mother-daughter (α-α) correlations for unambiguous isotopic assignment. Above all, it compares the behavior of the transactinide element with that of the lighter homologs zirconium (Zr) and hahnium (Hf) under identical conditions. It has not yet been efficient enough, however, to measure K_d values. This has only been achieved with improved techniques that have been developed more recently.

Another first-generation experiment by Hulet et al. [19], testing the chloride complexation of Rf, made use of computer automation to perform all chemical manipulations rapidly, to prepare α sources, and to conduct α spectroscopy. An extraction chromatographic method was chosen to investigate chloride complexation in high concentrations of hydrochloric acid (HCl). The extraction columns contained an inert support loaded with trioctyl-methylammonium chloride (Aliquat 336), since anionic chloride complexes formed in the liquid phase are strongly extracted into this ammonium compound. Such complexes are formed in 12 M HCl by the group-4 elements and are extracted, whereas group-1 through group-3 elements, including the actinides, are not appreciably extracted. Thus, these latter radionuclides were eluted from the column with 12 M HCl, while Zr and Hf, and Rf were extracted and subsequently eluted with 6 M HCl, in which chloride complexation is less favored. The results showed that the chloride complexation of Rf is consistently stronger than that of the trivalent actinides and is similar to that of Hf. No K_d value was determined in this "early" experiment.

For Rf in liquid phases, early experiments exploited the complexing with α-HiB [18] and the formation of chloride anions [19] and thus confirmed a behavior radically different from that of the heavy actinides. Although these were key experiments demonstrating that a new transition element series, the 6d-electron series, begins with $Z = 104$, none of these experiments provided detailed information on Rf chemistry.

3.2. Recent experiments with automated rapid chemical separation systems

Extensive series of detailed investigations were made possible by the development of computer-controlled automated systems that have greatly improved the ability to perform rapidly and reproducibly large numbers of chromatographic separations on miniaturized columns and to systematically vary ligand concentrations, thus allowing determining the stoichiometry of the eluted species. The experiments with automated devices have produced detailed and sometimes surprising results that called for a detailed theoretical modeling of the chemical properties with improved quantum-chemical calculations. On the other hand, several series of manually performed separations in liquid phases were also performed. Due to some experimental drawback in the manual separations, however, we rather concentrate on results obtained with automated systems that are summarized in Table 1.

Table 1. Experimental results obtained with automated rapid chemical separation systems. Assumed chemical species studied with elements 104 (Rf) through 106 (Sg), applied separation methods, adsorption sequences on the column, and references are indicated; CIX: cation-exchange chromatography, AIX: anion-exchange chromatography. For reversed-phase chromatography, the extractants are given; Aliquat 336: trioctyl-methylammonium chloride, TBP: tributyl-phosphate, TOPO: trioctylphosphine oxide, TiOA: triisooctyl amine, DIBC: diisobutyl carbinol.

Element	Assumed chemical species (transactinide element)[1]	Separation method	Adsorption sequence	Reference
Rf (Z = 104)	$[RfCl_6]^{2-}$	Aliquat 336	Rf ≈ Hf, Rf > An	Hulet et al. [19]
	$[RfCl_6]^{2-}$	AIX	Rf > Zr > Hf	Haba et al. [20]
	$RfCl_4(TBP)_2$	TBP	Zr > Hf > Rf	Günther et al. [21]
	$RfCl_4(TBP)_2$	TBP	Zr > Hf ≈ Rf	Haba et al. [22]
	$RfCl_4(TOPO)_2$	TOPO	Zr > Hf ≥ Rf	Toyoshima et al. [23]
	$[RfF_n]^{4-n}$	CIX	Th > Rf > Zr ≈ Hf	Strub et al. [24]
	$[RfF_n]^{4-n}$	CIX	Th > Rf > Hf ≥ Zr	Ishii et al. [25,26]
	$[RfF_n]^{4-n}$	AIX	Zr ≈ Hf > Rf	Strub et al. [24]
	$[RfF_6]^{2-}$	AIX	Zr ≈ Hf > Rf	Haba et al. [27]
	$[RfF_6]^{2-}$	AIX	Zr ≈ Hf > Rf	Toyoshima et al. [28, 29]
	$[Rf(HSO_4)_6]^{2-}$	CIX	Th > Rf > Hf ≥ Zr	Li et al. [30]
Db (Z = 105)	Db^{5+} - α-HiB	CIX	Db ≈ Nb ≈ Ta ≈ Pa	Schädel et al. [31]
	$[DbOCl_4]^-$ /$[Db(OH)_2Cl_4]^-$	TiOA	Db ≈ Nb ≈ Pa < Ta	Kratz et al. [32], Zimmermann et al. [33]
	$[DbOBr_5]^{2-}$	DIBC	Pa > Nb > Db	Gober et al. [34]
	$[DbCl_6]^-$	Aliquat 336	Pa > Nb ≥ Db > Ta	Paulus et al. [35]
	$[DbF_6]^-$	Aliquat 336	Db ≈ Nb ≈ Ta > Pa	Paulus et al. [35]
	$[DbF_6]^-$	AIX	Ta ≈ Nb > Db ≥ Pa	Tsukada et al. [36]
	$[DbOF_4]^-$	AIX	Ta > Db ≈ Nb ≈ Pa	Kasamatsu et al [37]
Sg (Z = 106)	$[SgO_2F_3(H_2O)]^-$/SgO_2F_2	CIX	Sg ≈ W	Schädel et al. [38, 39]
	$[SgO(OH)_3(H_2O)_2]^+$	CIX	Sg > W	Schädel et al. [40]

[1]Under identical conditions species of the light homologs can be different leading to differences in the chemical behavior.

[2]An = actinide element

As shown in Fig. 1, the liquid-phase experiments with the transactinide elements are carried out on the basis of the following steps: i) synthesis of a specific isotope of a transactinide element, ii) rapid transport of this nuclide to chemical separation devices by a gas-jet transport technique, iii) fast chemical characterization that includes dissolution in an aqueous solution containing inorganic/organic ligands for complex formation, iv) preparation of a sample suitable for nuclear spectroscopy (α-spectroscopy) which usually requires the evaporation of aqueous solution to dryness, and v) detection of nuclides through their characteristic nuclear decay properties for unambiguous identification. For characterization of the transactinide elements, recent partition experiments have been conducted using the automated rapid ion-exchange separation apparatus ARCA II (Automated Rapid Chemistry Apparatus) with a miniaturized computer-controlled liquid chromatography system [41] and AIDA (Automated Ion-exchange separation apparatus coupled with the Detection system for Alpha spectroscopy) [42]; AIDA consists of ARCA II and an automated on-line α-particle detection system. AIDA enables cyclic discontinuous column

chromatographic separations of short-lived nuclides in liquid phases and automated detection of α-particles within a typical cycle time of 60 s.

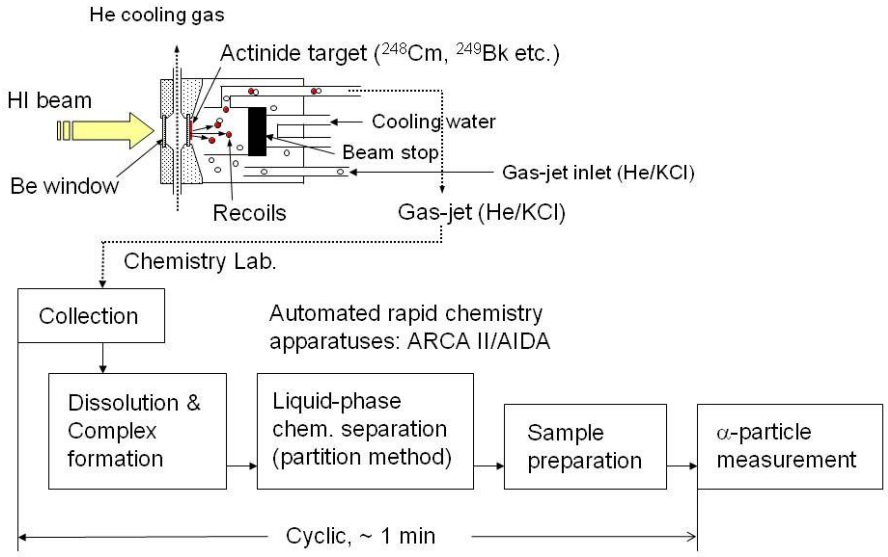

Fig. 1. Flow scheme of liquid-phase experiments with transactinide elements. Adapted from [11].

As mentioned before, the experimental approach generally involves comparative studies on the chemical properties of the transactinide elements with those of their lighter homologs and pseudo-homologs; i.e., elements with at least partially similar chemical properties but placed in a different group of the Periodic Table. Thus, all chemical experiments on the transactinide elements should be conducted together with their lighter homologs under identical conditions. In the following, we present typical experimental procedures as applied in Rf chemistry with the AIDA system. For the production of Rf, such as ^{261}Rf, and its homologs Zr and Hf, two different targets were used [43]; one is a mixed target of ^{248}Cm (610 μg cm^{-2} in thickness) and Gd (39.3%-enriched ^{152}Gd of 36 μg cm^{-2} in thickness) prepared by electrodeposition onto a 2.4 mg cm^{-2} Be foil for the simultaneous production of ^{261}Rf and 3.24-min ^{169}Hf via the ^{248}Cm(^{18}O, 5*n*) and Gd(^{18}O, *xn*) reactions, respectively. Another one is a ^{nat}Gd (370 μg cm^{-2} thickness) and ^{nat}Ge (660 μg cm^{-2} thickness) mixed target to produce ^{169}Hf and 7.86-min ^{85}Zr through the ^{nat}Gd(^{18}O, *xn*) and ^{nat}Ge(^{18}O, *xn*) reactions, respectively. The ^{nat}Gd was electrodeposited on a 2.7 mg cm^{-2} beryllium backing and then, on the resulting ^{nat}Gd target, ^{nat}Ge was deposited by vacuum evaporation. The reaction products recoiling out of the target were transported through a Teflon-capillary to the chemistry laboratory by a helium (He)/potassium chloride (KCl) gas-jet system.

A typical experimental procedure for studies of the anion-exchange behavior of Rf in hydrofluoric acid (HF) solution with AIDA is introduced in the following [27]. Reaction products recoiling from the target were transported by a He/KCl gas-jet to the collection site of AIDA. After collection for 125 s, the products were dissolved with 240 μL HF solution of various concentrations (1.9 - 13.9 M) and were fed onto the chromatographic column filled with the anion-exchange resin MCI GEL CA08Y (particle size of about 20 μm) at a flow rate of 0.74 mL min^{-1}. In the experiment, two different micro columns, 1.6 mm i.d. × 7.0 mm and 1.0 mm i.d. × 3.5 mm, were used to measure a wide range of distribution coefficients, K_d. The effluent was collected on a tantalum (Ta) disk as fraction 1 and was evaporated to dryness using hot He gas and a halogen heat lamp. Then, the remaining products in the column were stripped with 210 μL of 4.0 M HCl at a flow rate of 1.0 mL min^{-1}. The effluent was collected on another Ta disk and was evaporated to dryness as fraction 2. The pair of disks was automatically transported to the α-spectroscopy

station equipped with eight 600-mm^2 passivated ion-implanted planar silicon (PIPS) detectors. After the α-particle measurement, the γ-radiation of ^{169}Hf was monitored with Ge detectors to determine the elution behavior of Hf and its chemical yield. The anion-exchange experiments with ^{85}Zr and ^{169}Hf, produced from the Ge/Gd mixed target, were conducted under identical conditions as those with ^{261}Rf and ^{169}Hf. All effluents were collected in polyethylene tubes and were assayed by γ-ray spectroscopy. Each separation was accomplished within 20 s and the α-particle measurement started about 60 s after end of the collection of the products at the AIDA collection site. Typical for all group-4 elements, the chemical yield of Hf including deposition and dissolution efficiencies of the aerosols was approximately 60%.

To shorten the time for the sample preparation of α-ray sources, the newly developed rapid ion-exchange apparatus AIDA-II [11] was introduced; the apparatus is based on a continuous sample collection and evaporation of effluents, and successive α-particle measurement. The ion-exchange part is the same as that of AIDA. The AIDA-II was successfully applied for chemical experiments with Db [37].

4. Rutherfordium (Rf, *Z* = 104)

From the systematic investigation of ion-exchange chromatographic behavior of Rf, based on an atom-at-a-time scale, it has been found that the properties of Rf are quite similar to those of the group-4 homologs, Zr and Hf, in the formation of chloride, nitrate, and sulfate complexes, although there are some differences in complexation strength between Rf and the lighter homologs. On the contrary, fluoride complex formation of Rf is significantly different from that of the homologs. Here, we summarize the fluoride, chloride, sulfate, and organic complex formation of Rf.

4.1. Fluoride complex formation

Studies of the fluoride complexation of Rf have been extensively performed by Strub et al. [24] with ARCA II, and by Haba et al. [27], Toyoshima et al. [28, 29], and Ishii et al. [25, 26] with AIDA. As the fluoride anion, F^-, strongly coordinates with metal cations, strong ionic bonds are formed between metal cations and F^-. Thus, information about charge densities and ionic radii of the metal cations can possibly be obtained through studies of the fluoride complex formation. In addition, the fast reaction kinetics of the fluoride complex formation is an advantage when studying the chemical behavior of short-lived nuclides.

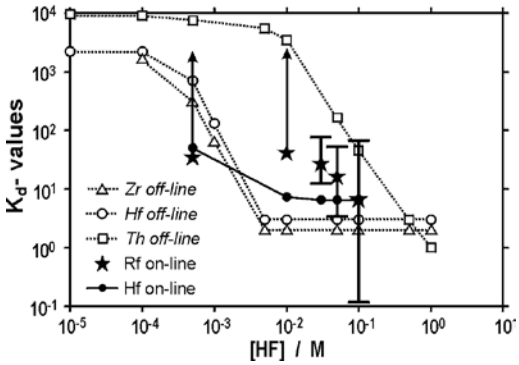

Fig. 2. K_d values (mL g^{-1}) of Zr, Hf, Th, and Rf on the cation-exchange resin, Aminex A6, in 0.1 M HNO_3 at various HF concentrations. Off-line data are shown for Zr, Hf, and Th, and on-line data for Rf and Hf. Taken from [9].

Strub et al. conducted Rf experiments with ARCA II at the Philips Cyclotron, Paul Scherrer Institute (PSI) [24]. The results of the on-line experiments with Rf and Hf on cation-exchange columns are given

in Fig. 2 together with the results of the off-line batch experiments. The on-line data for Hf are consistent with the off-line data. It is seen that the decrease of the K_d values for Rf occurs between 0.01 M HF and 0.1 M HF, i.e., at one order of magnitude higher HF concentrations than for Zr and Hf. Under the given conditions, the behavior of Rf is intermediate between that of its pseudo-homolog Th and that of group-4 elements Zr and Hf.

Further studies of the fluoride complexation of Rf have been performed with AIDA at the JAEA tandem accelerator facility [25-29]. Figure 3 depicts the K_d values for Rf, Zr, and Hf as a function of the concentration of HF_2^-, $[HF_2^-]$, by taking the dissociation of HF [44] into account. As shown in Fig. 3, the K_d values of the group-4 elements decrease linearly with $[HF_2^-]$ in a log K_d vs. log $[HF_2^-]$ plot. This feature is explained as the displacement of the metal complex from the binding sites of the resin by the counter anion HF_2^- according to the following equation [11, 27],

$$R_n\text{-}MF_{4+n} + n \cdot HF_2^- \rightleftarrows n \cdot R\text{-}HF_2 + MF_{4+n}^{n-} \quad (6)$$

(M = Rf, Zr, and Hf), where R denotes the resin. It should be noted here that the slopes for Zr and Hf are clearly –3 (dashed line), while that for Rf is significantly different, i.e., -2 (solid line). This implies that Rf is likely to be present as the hexafluoro complex, $[RfF_6]^{2-}$, similar to the well-known $[ZrF_6]^{2-}$ and $[HfF_6]^{2-}$ at lower concentration of HF, while Zr and Hf are likely to be present in the form of the heptafluoro complexes, $[ZrF_7]^{3-}$ and $[HfF_7]^{3-}$, as suggested in [45, 46].

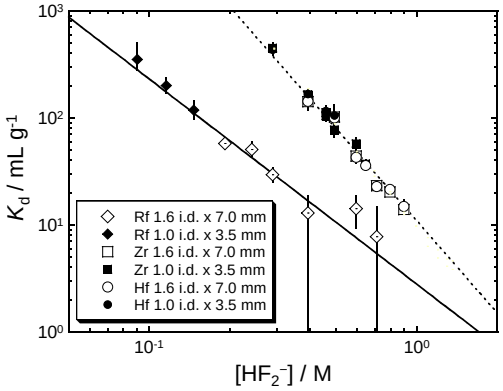

Fig. 3. Distribution coefficients (K_d) for Rf, Zr, and Hf obtained with two different size chromatographic columns filled with the anion-exchange resin CA08Y as a function of HF_2^- concentration, $[HF_2^-]$. In the inset, the column sizes for each experiment are indicated. Taken from [11].

Toyoshima et al. studied further the fluoride complexation of Rf in mixed HF/HNO_3 solutions using solution of lower HF concentration [29]. The anion-exchange behavior of Rf in the concentration ranges of 0.0054 - 0.74 M HF and of 0.010 - 0.030 M HNO_3 was investigated to clarify the type of anionic fluoride complex of Rf and to evaluate equilibrium constants of its formation reactions. The K_d values were systematically measured as a function of the concentration of the fluoride ion $[F^-]$ and of the nitrate ion $[NO_3^-]$. The formation of an anionic fluoride complex of Rf is interpreted in detail by taking into account chemical equilibria of anion-exchange reactions and of formation reactions of fluoride complexes and comparing those with the ones of the homologs Zr and Hf. The upper limit of formation constants for the fluoride complexes of Rf were experimentally evaluated for the first time. Figure 4(a) shows the variation of the K_d values for Rf, Zr, and Hf as a function of $[NO_3^-]$ at a constant $[F^-]$ of 3.0×10^{-3} M. The K_d values of Zr and Hf obtained in batch experiments are plotted by open squares and open triangles, respectively. The K_d values of Zr and Hf obtained in on-line column chromatographic experiments are

depicted by closed squares and closed triangles, respectively. The K_d values of Zr and Hf measured under dynamic conditions with the columns are in good agreement with those obtained under the static ones in batch experiments, indicating that all chemical reactions involved in the rapid chromatography studies attained equilibrium. It is found that the K_d values of Zr and Hf are identical with each other and the logarithmic values of K_d linearly decrease with the logarithmic increase of $[NO_3^-]$ with a slope of -2.0 ± 0.1, as indicated by the dashed line. The evaluated K_d values of Rf are indicated by closed circles. As shown in Fig. 4(a), at any given $[NO_3^-]$ the K_d values of Rf are much smaller than those of Zr and Hf, and they smoothly decrease with increasing $[NO_3^-]$ with the slope of -2.2 ± 0.2, as indicated by the solid line. The results indicate that, at constant $[F^-]$ of 3.0×10^{-3} M, anionic complexes of Rf, Zr, and Hf are present as $[MF_6]^{2-}$ (M = Rf, Zr, and Hf) [29].

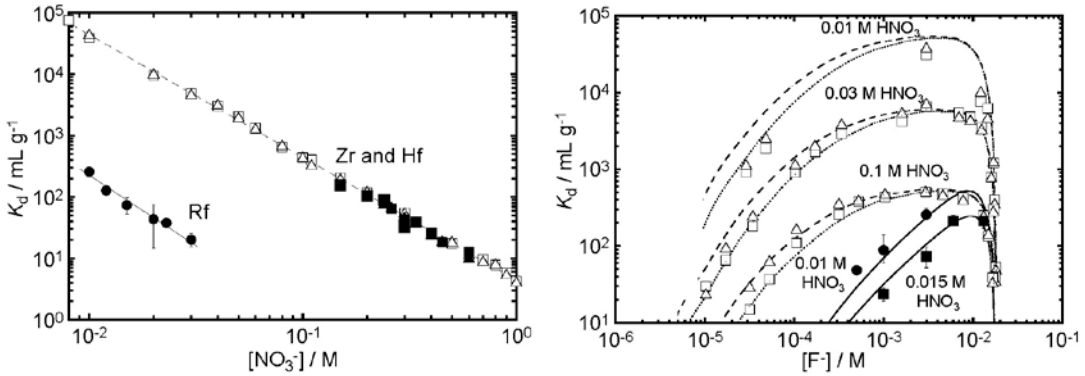

Fig. 4. (a) Distribution coefficients, K_d, of Zr and Hf measured under static conditions and those of Zr, Hf, and Rf from column chromatography as a function of the equilibrated concentration of NO_3^-, $[NO_3^-]$, at the fixed fluoride ion concentration, $[F^-] = 3.0 \times 10^{-3}$ M. Linear relationships of the log K_d vs. log $[NO_3^-]$ for Rf and the homologs are indicated by the solid and dashed lines, respectively. Adapted from [29]. (b) Variation of the K_d values of Zr and Hf (open symbols) obtained under static conditions and of Rf (closed circles) in column chromatography as a function of the equilibrated concentration of F^-, $[F^-]$. Values for Zr and Hf are shown for $[HNO_3] = 0.01$, 0.03, and 0.1 M, while those for Rf are shown for $[HNO_3] = 0.01$ and 0.015 M. The solid, broken, dash-dotted, and dotted curves are theoretical calculations of K_d values. Adapted from [29].

Figure 4(b) shows the variation of the K_d values for Rf, Zr, and Hf as a function of $[F^-]$. The K_d values of Zr and Hf measured under static conditions at $[HNO_3] = 0.01$ M, 0.03 M, and 0.1 M are represented. The K_d values for Rf at $[HNO_3] = 0.01$ M and 0.015 M are depicted by closed circles. The K_d values of Zr and Hf are close to each other; they begin to increase at around $[F^-] = 1 \times 10^{-5}$ M, gradually reaching constant K_d values between 10^{-4} - 10^{-3} M, and steeply decrease beyond $[F^-] = 5 \times 10^{-3}$ M. In contrast to the behavior of Zr and Hf at $[HNO_3] = 0.01$ M, the K_d values of Rf are about three orders of magnitude lower and they increase at 5.0×10^{-4} to 6.0×10^{-3} M. The solid, broken, dash-dotted, and dotted curves in Fig. 4(b) are results of theoretical calculations in which the log K_d is evaluated based on the formation constants K_n (n = 1 - 6) in fluoride complex formation and equilibrium constants in the anion-exchange process [29]. From this analysis, it is concluded that the maximum possible value of the formation constant K_6 for Rf is at least one order of magnitude smaller than those for Zr and Hf. This clearly demonstrates that the formation of the hexafluoro complex of Rf is much weaker than those of the homologs Zr and Hf [29].

The much weaker complexation of Rf by the fluoride ion is apparent when compared to that of its homologs. A qualitative explanation comes from the Hard Soft Acid Base (HSAB) concept [47-49]. The small fluoride anions are hard donors and prefer the smaller acceptor ions Zr^{4+} and Hf^{4+}: both having a

very similar radius. The larger (softer) Rf acceptor ion tends to prefer larger (softer, more polarizable) donor ligand ions like Cl^-.

The cation-exchange behaviour of Rf has been thoroughly studied in HF/HNO_3 mixed solution together with its lighter group-4 homologs Zr and Hf, and the tetravalent pseudo-homolog Th [25, 26]. The results by Ishii et al. confirm those from earlier investigation by Strub et al. [24] and they are in agreement with the interpretation of the anion-exchange studies mentioned above. The cation-exchange studies demonstrate that the K_d of Rf in HF/0.10 M HNO_3 decreases with increasing concentration of the fluoride ion [F^-], as shown in Fig. 5. This resembles the behavior of the homologs, indicating the consecutive formation of fluoride complexes of Rf. It is also ascertained that at these very low F^- concentrations the fluoride complex formation of Rf is significantly weaker than that of Zr and Hf, but it is stronger than that of Th. The sequence of adsorption strength on the cation-exchange resin is Zr ≤ Hf < Rf < Th at any given [F^-] [25, 26]. The observed K_d sequence of Zr ≤ Hf < Rf among the group-4 complexes is in agreement with that predicted theoretically in [50]. Here, free energy changes of the complex formation reactions were determined on the basis of fully relativistic density functional theory calculations of various hydrated and hydrolyzed fluoride complexes of Zr, Hf, and Rf. It was shown that at lower HF concentrations and 0.1 M HNO_3, the complex formation occurs preferentially from the hydrolyzed species. The strengths of the formed complexes is predicted as Zr ≥ Hf > Rf. This causes the following trend in the K_d values: Zr ≤ Hf < Rf.

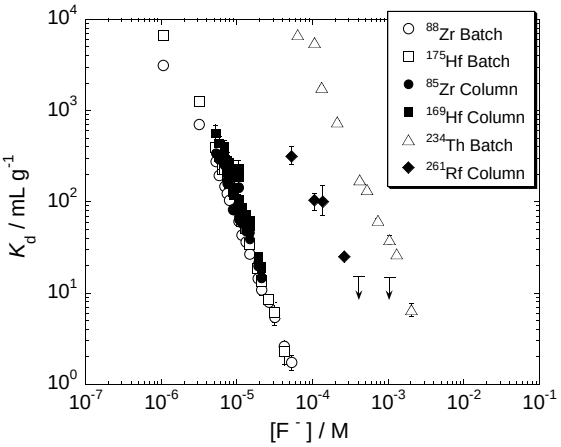

Fig. 5. Variation of the K_d values of Rf, Zr, Hf, and Th on the cation-exchange resin CK08Y in 0.10 M HNO_3 depending on [F^-]. Open symbols indicate data obtained in batch experiments, while solid ones show those from column separation [25, 26]. Taken from [11].

It was also shown in [50] that the electrostatic interaction plays a dominant role in the energies of the complex formation. Due to a predominantly electrostatic interaction, a correlation between crystallographic ionic radii (IR) [51] and the strengths of the formed complexes appears quite natural. The IR values of the group-4 elements with the coordination number of 6 are as follows [51]: Zr (72 pm) ≈ Hf (71 pm) < Rf (76 pm) [52] << Th (94 pm). In this particular case, this nicely correlates with the sequence in the complex formation Zr ≈ Hf > Rf > Th. Thus, assuming the same kind of interaction for all these elements, the present result is showing that the ionic radius of Rf^{4+} is in between those of Zr^{4+}/Hf^{4+} and Th^{4+}.

4.2. Chloride and sulfate complex formation

The adsorption behavior of Rf, Zr, and Hf on an anion-exchange resin as a function of HCl concentration was investigated by Haba et al. [20]. The adsorption behavior of Rf was quite similar to

those of the group-4 elements Zr and Hf. The adsorption of these elements rapidly increases with increasing HCl concentration above 7 M: typical for the anion-exchange behavior of the group-4 elements. This shows that anionic chloride complexes of the tetravalent Rf, Zr, and Hf are formed above 7 M HCl. An interesting feature is the observed adsorption sequence of these elements on the anion-exchange resin. This adsorption order reflects the strength of the chloride complex formation as Rf > Zr > Hf. The present result, however, contradicts the prediction with the relativistic molecular density-functional calculations by Pershina et al. where the sequence of the chloride complex formation is expected to be Zr > Hf > Rf [50]. According to the HSAB concept, it is reasonable that the larger (softer) Rf acceptor ion prefers the larger (softer) donor ligand ion Cl^-.

Recently, Li et al. [30] investigated the sulfate complexation of Rf through cation-exchange chromatography in 0.15 − 0.69 M H_2SO_4/HNO_3 mixed solutions ($[H^+]$ = 1.0 M). The sulfate ion SO_4^{2-} is a strong complexing ligand for group-4 elements. Its strength to form complexes with Zr and Hf is intermediate between those of F^- and Cl^- ions, i.e., $F^- > SO_4^{2-} >> Cl^- \geq NO_3^-$ [53]. It is of great interest, therefore, to study the sulfate complex formation of Rf to clarify whether it is similar to or significantly different from those of the lighter homologs Zr and Hf. The results clearly showed that the K_d values of Rf on the cation-exchange resin decrease with an increase of $[HSO_4^-]$. This indicates a successive formation of Rf sulfate complexes. Despite of some open questions concerning the kinetics in this experiment [30], it demonstrates that Rf has a much weaker tendency to form sulfate complexes than Zr and Hf. The formation strength of the Rf sulfate complex was intermediate between the fluoride and chloride complexation; a similar trend was observed for Zr and Hf. Experimental results are in good agreement with theoretical predictions based on relativistic electronic structure density functional theory calculations [54]. According to these predictions, Rf should have a much weaker preference for complex formation than Zr and Hf over the entire range of acid concentrations. Theoretical calculations show that the lower stability of the Rf complexes is due to the smaller ionic contribution to the chemical bond. This is caused by the relativistic stabilization of the 7s orbital, as well as the destabilization and spin-orbit splitting of the 6d orbitals. It is also in agreement with the larger ionic radius of Rf (76 pm) [52] in comparison with those of Zr (71 pm) and Hf (72 pm) [51]. Further, all results from systematic studies with ARCA II and AIDA about the complex formation of Rf with inorganic ligands can qualitatively be interpreted by the HSAB concept [47-49].

4.3. Extractions with tributylphosphate (TBP), trioctylphosphine oxide (TOPO), and dibutyl-phosphoric acid (HDBP)

The extraction behavior of Rf into tributylphosphate (TBP) from hydrochloric acids has been studied together with those of the lighter group-4 elements Zr and Hf by Günther et al. [21] and Haba et al. [22]. The extractability of these elements into TBP was investigated under identical condition in HCl by reversed-phase extraction chromatography. As shown in Fig. 6, the extractions of Rf, Hf, and Zr into the TBP resin increase steeply with increasing HCl concentration, and the order of extraction is Zr > Hf ≈ Rf [22].

The TBP extraction of the group-4 elements in HCl is expressed by the following chemical equations:

$$[M(H_2O)_8]^{4+} + 4Cl^- \rightleftarrows MCl_4 + 8H_2O, \quad (7)$$

$$MCl_4 + 2TBP(aq) \rightleftarrows MCl_4(TBP)_2(org). \quad (8)$$

Coordinated H_2O molecules are stepwise replaced by Cl^- when increasing the HCl concentration and the subsequently formed neutral tetrachloride complex is extracted into the organic phase as $MCl_4(TBP)_2$. Thus, the extractability of group-4 elements into TBP is expected to depend on the chloride complex formation and on the stability of the TBP complex. From the anion-exchange experiments of Rf in 4.0 –

11.5 M HCl [20] and the detailed structural studies on the Zr and Hf complexes in HCl by the EXAFS spectroscopy [55], it was deduced that Rf forms the same complexes as Zr and Hf: $[Rf(H_2O)_8]^{4+} \rightarrow [RfCl_6]^{2-}$, and that the affinity of Cl^- for these metal ions follows the order of Rf > Zr > Hf. The smaller extractability of Rf in the TBP extraction then would indicate that the stability of the TBP complex of Rf chloride, $RfCl_4(TBP)_2$, is weaker than those of Zr and Hf.

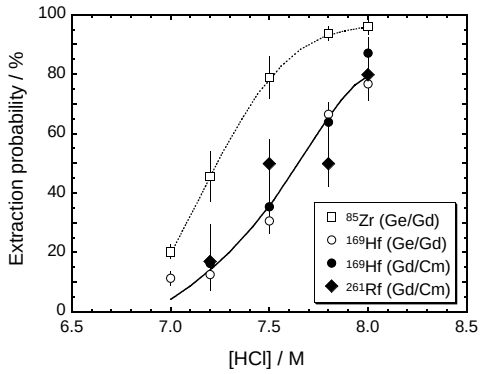

Fig. 6. Extraction probability of Rf, Zr, and Hf on a 20-wt.% TBP/CHP20Y resin as a function of HCl concentration. The data for ^{261}Rf and ^{169}Hf obtained from the Cm/Gd target are shown by closed diamonds and closed circles, respectively, while those for ^{85}Zr and ^{169}Hf from the Ge/Gd target are by open squares and open circles, respectively. The data for Zr and Hf are connected by a dotted curve and a solid curve, respectively. Taken from [11].

The extraction behavior of Rf into trioctylphosphine oxide (TOPO) from 2.0 - 7.0 M HCl solutions was also investigated together with Zr and Hf [23]. TOPO has a chemical structure similar to that of TBP but it has a higher basicity value as a donor (8.9) than that of TBP (0.16) [56, 57]. The effect of the basicity of the organophosphorus compounds on the stability of the formation of a Rf complex was examined by comparing the extraction sequence of the group-4 elements into TOPO with that into TBP previously studied [22]. The extraction order of the group-4 elements Rf, Zr, and Hf into TOPO was Zr > Hf ≥ Rf; the stability of the $RfCl_4(TOPO)_2$ complex is lower than those of the corresponding species of Zr and Hf. An effect of the basicity on the formation of the TOPO and TBP complexes was not clearly observed in the extraction sequence among Rf, Zr, and Hf in HCl [23].

The fast centrifuge system SISAK, Short-lived Isotopes Studied by the AKUFVE-technique, where AKUFVE is a Swedish acronym for an arrangement of continuous investigations of distribution ratios in liquid extraction, was applied to perform continuous liquid-liquid extraction and detection of short-lived Rf using small-volume centrifuges and a liquid-scintillation detection system. SISAK, employed to extract 4-s ^{257}Rf produced in the ^{208}Pb(^{50}Ti, *n*) reaction, was coupled to the kinematic recoil separator BGS (Berkeley Gas-filled Separator) at the Lawrence Berkeley National Laboratory (LBNL) 88-inch cyclotron [58, 59]. Recoiling ^{257}Rf, pre-separated from the primary beam and nuclear reaction by-products, was thermalized in a stopping-gas cell termed Recoil Transfer Chamber (RTC) and was transferred to SISAK through the He/KCl gas-jet system. Figure 7 shows a schematic diagram of the SISAK set-up. Products delivered to the apparatus with the aerosol gas-jet are mixed with 6 M HNO_3 to dissolve the aerosol-laden products, and the carrier gas is removed in a degasser centrifuge. The aqueous solution is mixed with an organic solvent, 0.25 M dibutyl-phosphoric acid (HDBP) in toluene. Here Rf is extracted as a Rf nitrate-HDBP compound into the organic toluene. Then the organic phase is washed with 2 M $NaNO_3$ to remove acidic solution. A scintillation cocktail containing the mixture of the organic solvent and the scintillator ingredients is then fed to a detector system to perform liquid scintillation α-spectroscopy for the flowing cocktail. The extraction behavior of Rf was similar to that of the homologs Zr and Hf [58]. The above pilot experiment demonstrated that the SISAK system in combination with

liquid scintillation detectors can be used for the investigation of chemical properties of the transactinide elements.

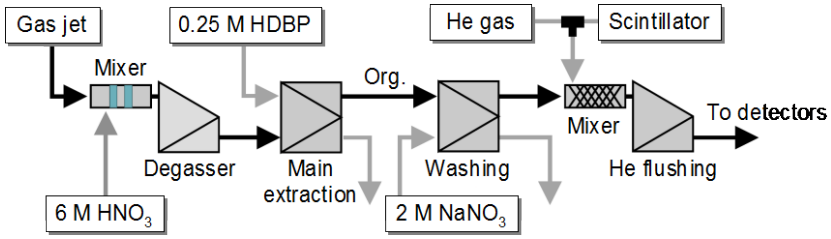

Fig. 7. Schematic diagram of the SISAK liquid-liquid extraction system. Adapted from [58].

5. Dubnium (Db, Z = 105)

First studies of the liquid phase chemistry of Db were conducted manually in 1987 by Gregorich et al. [60]. 34-s ^{262}Db was produced in the irradiation of ^{249}Bk with ^{18}O ions at the LBNL 88-inch cyclotron. Like the homologs niobium (Nb) and tantalum (Ta), Db was adsorbed on a glass surface upon fuming with nitric acid. The other chemical separation attempted in [60] involved the extraction of anionic fluoride species into methyl isobutyl ketone (MIBK). The extraction system with 3.8 M HNO_3 and 1.1 M HF as the aqueous phase and MIBK as the organic phase was chosen because MIBK had been found to be an ideal solvent for the rapid preparation of α sources by evaporation. Under these conditions, Ta was extracted into MIBK nearly quantitatively, while Nb was extracted to only a small extent. It was found that Db is not behaving chemically like its lighter homolog Ta. The non Ta-like behavior of Db might indicate that Db forms polynegative anions like $[DbF_7]^{2-}$ under the chosen conditions.

To investigate this unexpected finding and more facets of Db chemistry, a large number of automated separations were conducted with ARCA II [31-35]. In the first experiments, extraction chromatography separations with the liquid anion-exchanger triisooctyl amine (TiOA) on an inert support were performed [31, 32]. TiOA extracts all group-5 elements including the pseudo-homolog protactinium (Pa), irrespective of the formation of mono- or polynegative anions, from HCl solutions above 10 M. At lower concentrations, selective back extractions can distinguish the chemical behavior of Nb, Ta, Pa, and Db. Kratz et al. [32] showed that element 105 (Db) extracts into the TiOA on the chromatographic columns in ARCA II from 12 M HCl / 0.02 M HF as do Nb, Ta, and Pa, due to the formation of anionic halide complexes. Db showed a striking non Ta-like behavior and it followed, at all HCl concentrations below 12 M, the behavior of its lighter homolog Nb and that of its pseudo-homolog Pa. From this similarity, it was concluded that the complex structure of Db was $[DbOCl_4]^-$ or $[Db(OH)_2Cl_4]^-$, and the preferential formation of oxyhalide complexes of Db was also predicted theoretically [61].

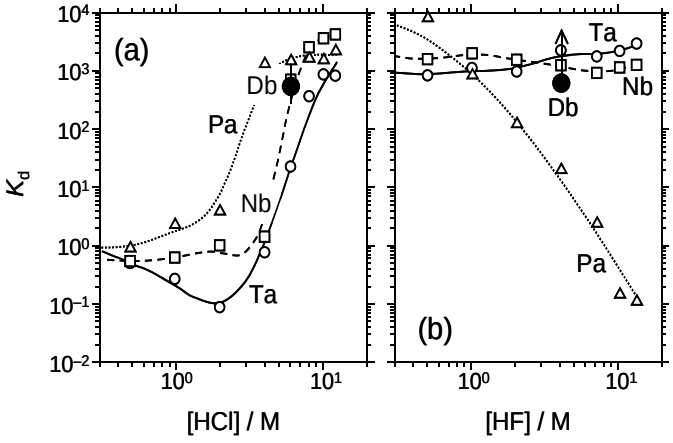

Fig. 8. (a) Variation of the K_d values (mL g^{-1}) of Pa, Nb, and Ta from HCl solutions into Aliquat 336/HCl. The distribution coefficient, K_d, of Db in 6 M HCl (with error bars encompassing the 68% confidence limit) is indicated by the bold dot. Adapted from [35]. (b) Extraction behavior of Pa, Nb and Ta from HF solutions in Aliquat 336/HF. The lower limit for the K_d value of Db in 4 M HF (representing the 68% confidence limit) is indicated by the bold dot with the arrow. Adapted from [35].

Amine extraction experiments with the quaternary ammonium salt Aliquat 336 of group-5 elements were systematically performed by Paulus et al. [35]. Chromatographic column separations with ARCA II were developed to study separately the fluoride and chloride complexation of Db. 1307 experiments were carried out with Db with a cycle time of 50 s. In the system Aliquat 336/HCl, a K_d value (mL g^{-1}) of

438^{+532}_{-166} for Db in 6 M HCl was deduced which is close to that of Nb and differs from the values for Pa and Ta: see Fig. 8(a). Thus, the extraction sequence Pa > Nb ≥ Db > Ta is established exactly as theoretically predicted [62, 63]. In the system Aliquat 336/HF, the result is depicted in Fig. 8(b). The interpretation of these results indicates that the amine extraction behavior of Db halide complexes is always close to that of its lighter homolog Nb. In HF solution, the behavior of Db differs mostly from that of Pa, while it differs considerably from both Pa and Ta in HCl; see Fig. 8(b).

The anion-exchange behavior of Db produced in the ^{248}Cm(^{19}F, 5*n*)^{262}Db reaction [64] at the JAEA tandem accelerator was investigated by Tsukada et al. [36] together with the homologs Nb and Ta, and the pseudo-homolog Pa, with the anion-exchange resin CA08Y in 13.9 M HF solution. The experimental procedures with AIDA were basically the same as those in the Rf experiments. The results indicated that the adsorption of Db on the resin was significantly different from that of the homologs and that the adsorption decreases in the sequence Ta ≈ Nb > Db ≥ Pa. In solutions with lower fluoride ion concentration, Kasamatsu et al. ascertained the well-known significantly different anion-exchange behavior between Nb and Ta in mixed HF/HNO_3 [37]. They measured the K_d value of Db in 0.31 M HF/0.10 M HNO_3 solution ([F^-] = 0.003 M), where Nb and Ta form $[NbOF_4]^-$ and $[TaF_6]^-$, respectively. Reaction products recoiling out of the target were continuously transported by the He/potassium fluoride (KF) gas-jet from the target chamber to the collection site of a newly developed rapid ion-exchange separation apparatus, AIDA-II [11]. The K_d value of Db was determined and it was found that the adsorption of Db on the resin is considerably weaker than that of Ta and is similar to that of Nb and Pa: see Fig. 9. As discussed in [65], this result suggests that Db forms a fluoro-oxo complex $[DbOF_4]^-$, like Nb, but not $[DbF_6]^-$, like Ta. Note that the K_d value of Db is also close to that of Pa that forms $[PaOF_5]^{2-}$ and/or $[PaF_7]^{2-}$ [65-67]. The formation of complexes such as $[DbOF_5]^{2-}$ and $[DbF_7]^{2-}$ could also be suggested for Db. To unequivocally clarify the fluoride complexation of Db, further systematic study of Db as a function of [F^-] and [NO_3^-] is required.

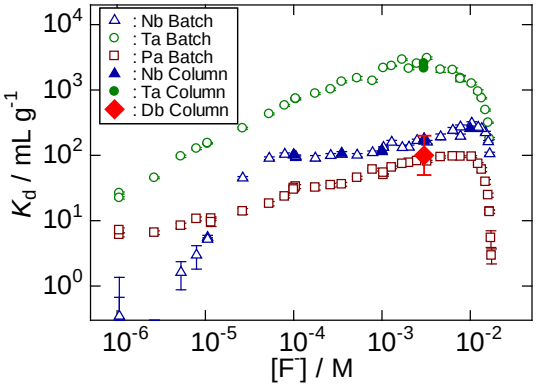

Fig. 9. Distribution coefficients, K_d, of Nb, Ta, Pa, and Db on the anion-exchange resin in HF/0.1 M HNO_3 depending on the fluoride ion concentration. Taken from [11].

Recently, chemical identification of Db as a decay product of element 115 produced in the reaction ^{243}Am + ^{48}Ca was performed [68-70]. A 32-cm^2 rotating target consisting of the enriched isotope ^{243}Am in the oxide form was bombarded by a 247-MeV ^{48}Ca beam at the U-400 cyclotron at the Flerov Laboratory of Nuclear Reactions (FLNR), Dubna, Russia. The recoiling reaction products were stopped in a 50 mm diameter Cu catcher foil. After the end of bombardment (EOB), a 7-10 μm thick layer of the Cu catcher was mechanically cut from the surface. The Cu was chemically processed to isolate Db and Rf, which are α-decay descendants of element 115; the layer was dissolved in 10 mL of conc. HNO_3. The resulting solution contained a large amount of Cu and unwanted reaction products. The group 4 and 5 elements

were separated from Cu through co-precipitation with $La(OH)_3$ by introducing ammoniumhydroxide and the La^{3+} carrier to the solution. The precipitate was dissolved in 2 M HNO_3, which was loaded onto the strongly acidic cation exchanger Dowex 50 × 8 and subsequently washed with 1 M HF. The group 4 and 5 elements were eluted from the column, while the actinides remained adsorbed on the column. Then the effluent was evaporated and deposited onto a polyethylene foil with subsequent drying in a stream of warm He gas. All procedures starting from the EOB until the beginning of detector measurements took 2-3 h [68-70].

In the eight irradiation samples, 15 spontaneous fission, SF, events were detected within 174 h. A decay analysis resulted in a single component with a half-life of 32^{+11}_{-7} h that agrees with $T_{1/2}$ obtained in the separate physical experiment [71] within statistical errors. A cross section for the production of the long-lived SF nuclide from, presumably ^{243}Am(^{48}Ca, 3*n*)^{288}115, was reported to be about 4 pb [68-70]. Schumann et al. concluded that the observed nuclide forms a hydroxide in ammonium solution coprecipitating with $La(OH)_3$ and forms strong anionic fluoride complexes in HF solution, indicating that its chemical properties correspond to that of a group 4 or 5 element [69].

6. Seaborgium (Sg, *Z* = 106)

The first chemical separation and characterization of Sg in the liquid phase was performed by Schädel et al. [38, 39] using the isotope ^{265}Sg ($T_{1/2}$ = 7.4 s [72, 73]) produced in the reaction of ^{22}Ne with ^{248}Cm at GSI (Gesellschaft für Schwerionenforschung) UNILAC (UNIversal Linear Accelerator) (Today's knowledge on the decay of ^{265}Sg shows the presence of two states; one with a half-life of about 9 s and one with about 15 s [74, 75]). The nuclear reaction products were transported to ARCA II, dissolved in 0.1 M HNO_3/5 × 10^{-4} M HF, and separated on a cation-exchange resin. To probe the Sg behavior in comparison with its lighter group-6 homologs molybdenum (Mo) and tungsten (W), and with the pseudo-homolog uranium (U), 3900 identical separations were performed with a cycle time of 45 s. Three correlated mother-daughter (α-α) decays were observed that were assigned to the decay of ^{261}Rf and ^{257}No, as the descendants of ^{265}Sg; see Fig. 10. As the mother decays were not observed, it is important to note that ^{261}Rf and ^{257}No can only be observed if the mother, ^{265}Sg, passed through the column because group-4 elements and No are strongly retained on the cation-exchange columns. Most likely, the decay of ^{265}Sg was not observed because it decayed in the time interval between the end-of-separation and the start-of-measurement which was equivalent to four half-lives. That the columns really retained ^{261}Rf was demonstrated in an experiment where ^{261}Rf was produced directly in the ^{248}Cm(^{18}O, 5*n*) reaction at the PSI Philips cyclotron [24], and processed as in the Sg chemistry in 0.1 M HNO_3/5 × 10^{-4} M HF. ^{261}Rf did not elute from the column and was subsequently stripped from the column with 0.1 M HNO_3/10^{-1} M HF. From the observation of the three correlated α-decay chains of ^{265}Sg daughters it was concluded, that, for the first time, a chemical separation of Sg was performed in aqueous solution. Sg shows a behavior typical of a hexavalent element located in group 6 of the Periodic Table. It is different from that of the pseudo group-6 element uranium, which is fixed as UO_2^{2+} on the cation exchange column. Presumably, Sg forms $[SgO_2F_3(H_2O)]^-$ or the neutral species $[SgO_2F_2]$. However, due to the low fluoride concentration used, the anionic $[SgO_4]^{2-}$ ('seaborgate' in analogy to molybdate, $[MoO_4]^{2-}$, or tungstate, $[WO_4]^{2-}$) could not be excluded [39].

In order to clarify this situation, a second series of experiments with ARCA II was performed, which used pure 0.1 M HNO_3 leaving out the potential complexing agent HF [40]. In 4575 separations, and expecting five correlated events, only one candidate for an α-α correlation attributable to the ^{261}Rf-^{257}No pair was observed which had a 30% probability to be a random correlation. This result indicates that, in the absence of fluoride ions and contrary to a typical W-like behavior, there is no sorption of Sg on the cation exchange resin. This can be attributed to the weaker tendency of Sg to hydrolyze. Consequently, hydrolysis may stop at still cationic species, like $SgO(OH)_3(H_2O)_2^+$, instead of forming neutral or anionic complexes as Nb and W do. From this it seems plausible that, in the preceding experiment, F^- ions

participated in the complex formation leading to one of the above mentioned neutral or anionic fluoride complexes of Sg.

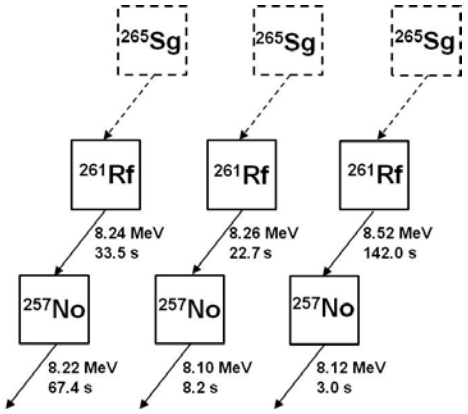

Fig. 10. Nuclear decay chains originating from ^{265}Sg after chemical separation with ARCA II. Taken from [10].

7. Electrochemical approach to the heaviest elements

Redox studies of the heaviest elements are expected to give valuable information on valence electronic states influenced by strong relativistic effects, such as oxidation states and redox potentials. Well established electrochemical approaches like cyclic voltammetry are, however, not available for the one atom-at-a-time chemistry of the heaviest elements. Thus, one needs to investigate redox properties of the heaviest elements based on the partition behavior of single atoms between two phases instead of measurements of electric currents from redox reactions.

A new apparatus for the study of electrochemical properties of the heaviest elements has been developed by Toyoshima et al. [76]. The apparatus is based on a flow electrolytic cell combined with column chromatography. The working electrode is made of a bundle of glassy-carbon fibers that is packed in a porous Vycor glass tube (4.8 mm i.d., 7 mm o.d., and 30 mm long) which works as an electrolytic diaphragm. The surface of the carbon fibers was chemically modified with Nafion® perfluorinated cation-exchange resin (Nafion® dispersion solution DE2020, Wako Chemicals). A platinum-mesh counter electrode was placed in the electrolyte pool to surround the glass tube. The potential on the working electrode was controlled using a potentiostat referring to the 1.0 M LiCl-Ag/AgCl electrode placed in the pool.

The apparatus was applied to the oxidation of No^{2+} by controlling the applied potential [77]. Toyoshima et al. successfully conducted the oxidation of single No^{2+} ions to the trivalent state No^{3+} in α-HiB solution. The isotope ^{255}No with a half-life of 3.1 min was synthesized in a nuclear reaction between ^{12}C ions and a ^{248}Cm target at the JAEA tandem accelerator. Nuclear reaction products recoiling out of the target were attached to KCl aerosols seeded in a He gas stream and then continuously transported to the chemistry laboratory through a Teflon capillary (2.0 mm i.d. × 25 m) within a few seconds. For 10 minutes, the transported products were deposited on a collection plate of AIDA. Then, the products were dissolved with 1080 μL of 0.1 M α-HIB (pH 3.9) and were subsequently fed through a thin Teflon tube into the electrochemical apparatus at a flow rate of 600 μL min^{-1}. The effluent including the fraction of No^{3+} from the column electrode was consecutively collected with a volume of 180 μL for each fraction on six separate Ta disks. The remaining products in the column that contain No^{2+} were stripped with 360 μL of 3.0 M HCl and were collected on two additional Ta disks. These eight samples were evaporated to

dryness using hot He gas and halogen heat lamps and were then transferred to the α-spectrometry station of AIDA. The above procedures were accomplished within 3 min and repeated numerous times to obtain sufficient statistics for the α-decay counts of ^{255}No.

Figure 11(a) shows the oxidation probability of No as a function of the applied potential, the probability defined as 100 × [No^{3+}] / ([No^{2+}] + [No^{3+}]), where [No^{2+}] and [No^{3+}] represent the radioactivities of ^{255}No measured in the 3.0 M HCl and 0.1 M α-HiB fractions, respectively. The oxidation reaction begins at about 0.7 V and is complete by 1.0 V. The formal redox potential of the $No^{3+} + e^- \rightleftarrows No^{2+}$ reaction corresponding to a half of the oxidation probability is evaluated to be approximately 0.75 V under the present conditions [77]. Recently, the reduction behavior of mendelevium (Md) was studied using the flow electrolytic chromatography apparatus. By application of the appropriate potentials on the chromatography column, the more stable Md^{3+} is reduced to Md^{2+}. The reduction potential of the $Md^{3+} + e^- \rightleftarrows Md^{2+}$ couple was determined to be -0.16 ± 0.05 V vs. a normal hydrogen electrode [78]; Fig. 11 (b). This new technical approach will open up new frontiers of the chemistry of the transactinide elements.

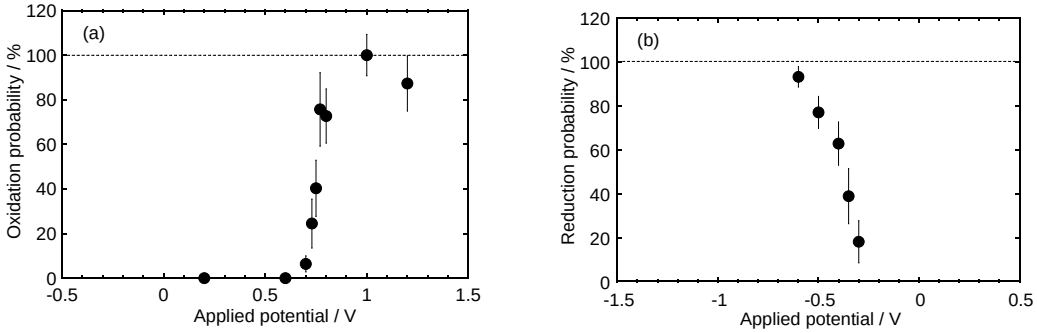

Fig. 11. (a) Oxidation probability of divalent No as a function of the applied potential. Adapted from [77]; (b) Reduction probabilities of Md in 0.1 M HCl. Adapted from [78].

8. Perspectives

In recent years, new technical and methodological developments were carried out, and are still ongoing, which provide a basis for future liquid-phase chemistry experiments. These have the potential to provide new insights into properties of the lighter transactinides and to push the frontier even beyond seaborgium. Often, a new quality can be reached by coupling liquid-chemistry devices to gas-filled recoil separators. In the following, we briefly outline some of the options using redox reactions and electrodepositions as an example as well as new approaches to provide better knowledge of the complex formation behavior of transactinides and to exploit chemistry as a tool to provide clean samples for deeper insights into nuclear properties.

It is highly interesting to perform electrochemical studies of the transactinide elements because advanced theoretical model calculations can provide quantitative predictions [79, 80]. Presently, preparations are under way to measure the redox potential of the hexavalent Sg [81]. In one approach, a complex and continuously working system is envisioned which consists of an electrochemistry apparatus for the potentially controlled Sg reduction [77, 78] connected to a separation device like SISAK [82] for the extraction, and a flow-through liquid-scintillation detection system [59]. By means of a newly designed interface [83], this shall be coupled with a recoil separator like GARIS (Gas-filled Recoil Ion Separator) at RIKEN [84]. In this future program, the ^{265}Sg nuclide produced in the ^{248}Cm(^{22}Ne, 5*n*)

reaction is planned to be pre-separated from the primary beam and nuclear reaction by-products by GARIS, followed by thermalization in a stopping-gas cell and transfer to the chemistry set-up through the He/KCl gas-jet system. After de-gassing, the products are fed into the electrochemistry apparatus to reduce the Sg^{6+} to the pentavalent or tetravalent state. Then, ions in the hexavalent and in a low oxidation state are separated from each other by solvent extraction in SISAK, and both streams of liquid will be assayed by α-spectrometry. If successful, this will give the first information on redox properties of a transactinide element.

The theoretical prediction of redox potentials of the group-6 elements Cr, Mo, W, and Sg by Kratz and Pershina [79, 80] had shown that Sg would be the first transactinide element in which a lower oxidation state than the one corresponding to the group number would be experimentally accessible. Therefore, Strub [85] performed first off-line experiments in which the lighter homologs Mo(VI) and W(VI) were reduced in acidic aqueous solutions such as 0.03 M HCl/5 × 10^{-5} M HF by passing these through a column filled with metallic aluminum (Al) at elevated temperatures. This allowed separating the hexavalent oxidation state anionic ions, $MoO_2F_3^-$ and $WO_2F_3^-$, from the reduced cationic species, presumably Mo(IV) and W(IV), on an anion or cation exchange column. Applying this technique, the non-reduced hexavalent $WO_2F_3^-$ was eluted first from a cation exchange column in 0.03 M HCl/5 × 10^{-4} M HF while the reduced species remained on the column and was stripped later with 4 M HCl/0.01 M HF. In the reduction reaction

$$WO_2F_3^- + 2H^0 + 2H^+ \rightleftarrows W(IV) + 2H_2O + 3F^-, \quad (9)$$

nascent hydrogen at the surface of the Al metal is likely to reduce the W(VI). The reduction did not work at room temperature. It required a temperature in excess of 65 °C and 90 °C to achieve a reduced fraction of 50% and 80%, respectively.

Elements 108–116 are expected to be partially very noble metals. Thus, at least for some elements with longer lived isotopes, their electrochemical deposition on suitable electrode materials from aqueous solutions could be an attractive method for their isolation. It is known that the potential associated with the electrochemical deposition of radionuclides in metallic form from solutions of extremely small concentration is strongly influenced by the choice of the electrode material. The experimentally observed "underpotential deposition" is reproduced by Eichler and Kratz [86] in a model in which the interaction between the micro-component *A* and the electrode material *B* is described by the partial molar adsorption enthalpy and entropy. By combination with the thermodynamic description of the electrode process, a potential is calculated that characterizes the process at 50% deposition:

$$E_{50\%} = E^0 - \frac{\Delta H(A-B) - T\Delta S_{\mathrm{vib}}}{nF} - \frac{RT}{nF} ln \frac{A_{\mathrm{m}}}{1000} \quad (10)$$

Here, $\Delta H(A-B)$ is the partial molar net adsorption enthalpy associated with the transformation of 1 mol of the pure metal *A* in its standard state into the state of 'zero coverage' on the surface of the electrode material *B*, ΔS_{vib} is the difference in the vibrational entropies in the above states, *n* is the number of electrons involved in the electrode process, *F* is the Faraday constant, and A_{m} the surface of 1 mol of *A* as a mono layer on the electrode material *B* [86]. For the calculation of the thermodynamic functions in Eq. 10, a number of models were used by Eichler and Kratz [86]. Calculations were performed for Ni-, Cu-, Pd-, Ag-, Au-, and Pt-electrodes and the micro components Hg, Tl, Pb, Bi, and Po, thus confirming the decisive influence of the choice of the electrode material on the deposition potential. For Pd and Au, particularly large and positive values of $E_{50\%}$ were obtained, much larger than the standard electrode potentials (Nernst potentials) tabulated for these elements. This makes these electrode materials the prime choice for practical applications. An application of the same model for superheavy elements still needs to

be done, but one can anticipate that the preference for Pd and Au will persist. The latter are metals in which, due to the formation of the metallic bond, almost or completely filled d orbitals are broken up so that the metals tend in an extreme way towards the formation of intermetallic compounds with sp-metals. The perspective is to make use of these metals in the form of a tape on which the transactinides are electrodeposited and the deposition zone is subsequently stepped between pairs of Si detectors for α and SF spectroscopy [87].

As already mentioned before, Schädel et al. studied the Sg chemistry [38-40] and they reported that Sg behaves like a typical group-6 element, but does not behave like its pseudo-homologue U. In addition, their experiment suggests a different trend in hydrolysis between Sg and its homologs. There are, however, still open questions concerning the hydrolysis and fluoride complexation of Sg. Thus, more detailed and statistically improved fluoride complex formation experiments of Sg are very attractive. The JAEA group at Tokai has already measured K_d values of the homologs of Sg as a function of the fluoride ion concentration in anion-exchange chromatography [88]. To conduct an experiment with short-lived ^{265}Sg produced at a low rate of the order of 10 atoms per hour [75], however, the development of a new rapid separation apparatus is required.

Continuous liquid-liquid extraction of short-lived radionuclides has traditionally been performed with the SISAK system consisting of static mixers and centrifuges for phase separation [82]. SISAK operates at flow rates of typically 1 mL s^{-1}. Thus, it produces large volumes of liquid waste that is difficult to treat or to dispose of. Therefore, it has been aimed to develop and use a further miniaturised extraction unit based on microtechnology and precision engineering to reduce the flow rate by at least two orders of magnitude. The accordingly developed MicroSISAK device [89] is a micro membrane extractor in which a micromixer element with 2 × 16 feed channels of 30 µm width followed by a 60 µm high mixing chamber is used for “interdigital mixing” of the aqueous and organic phase. Subsequent phase separation is achieved via hydrophobic Teflon membranes with a pore size of 1 µm. The MicroSISAK device has been tested and optimized with radiotracers of the group-4 elements Zr and Hf in the system H_2SO_4/trioctyl amine (TOA) in toluene. At a temperature of 58 ^{o}C and a flow rate of 0.2 mL min^{-1} of both phases, extraction yields of 87±3% were achieved. The transport time from the micromixer to the first Teflon membrane was in this case 3.9 s. It can be shortened to 1.56 s at a flow rate of 0.5 mL min^{-1}. Under similar conditions, the extraction yield of ^{99m}Tc milked from a ^{99}Mo generator in the system HNO_3/tetraphenyl arsonium chloride (TPAC) in chloroform was 83±3%. In an on-line experiment at the TRIGA Mainz reactor, short-lived Tc isotopes produced in the fission of ^{235}U with thermal neutrons were transported by the He/KCl gas-jet to the chemistry apparatus, deposited by impaction, dissolved in 0.01 M HNO_3/$KBrO_3$, and extracted into 10^{-4} M TPAC in chloroform in MicroSISAK. The separated phases were transported via capillaries to two separate flow-through cells positioned in front of two Ge detectors. The extraction yield determined as the ratio of the Tc γ-ray activities in both detectors was 76±1 %. With this experiment, it was demonstrated that MicroSISAK is in principle ready for an on-line experiment for the chemical characterization of the superheavy element, bohrium (Bh), element 107. However, the detection of α-particle activities by liquid scintillation counting still needs to be worked out.

Interesting perspectives arise from the observation of relatively long-lived isotopes of all elements from hassium (Z=108) to flerovium (Z=114) [90] first observed in the pioneering work at the FLNR. Mostly synthesized in ^{48}Ca induced reactions (^{26}Mg in the case of $^{269-271}$Hs) not only these directly produced isotopes are of interest but also the α-decay grand-grand-daughter nuclei in the rutherfordium to dubnium region some having half-lives of the order of one day. On the one hand, this makes chemical investigations of the heaviest element in the Periodic Table all the way up to flerovium conceivable. The chemistry of these elements should be extremely interesting due to the predicted dramatic influence of relativistic effects [6-8]. In addition, being able to investigate isotopes of Rf and Db with half-lives as long as a day opens up new perspectives for the application of new techniques which require longer times but provide deeper insights. However, for all these studies at first new technical developments are mandatory to cope with cross section in the range between 10 and 1 pb.

Chemistry experiments of the transactinide elements do not only focus on studies of the chemical properties of these elements to unravel the influence of relativistic effects on the electronic orbitals, they also provide clean samples for nuclear investigations with the great advantage of a unique signature in atomic number. In the recent years, not only experiments performed in the liquid-phase but predominantly those carried out in the gas-phase have significantly contributed to nuclear decay studies of neutron-rich nuclides and to the characterization of new nuclides, such as ^{263}Rf [91], ^{263}Db [92], ^{265,266}Sg [38, 93], ^{266,267}Bh [94], ^{269,270,271}Hs [95-98], ^{283}Cn [99, 100], ^{284}113 [101], and ^{288,289}Fl [102]. Liquid-phase techniques were also applied in the characterization of long-lived α-decay daughter nuclei which undergo spontaneous fission [69]. They showed the potential for a unique identification of the atomic number in liquid-phase experiments of transactinides.

The advantages of chemical techniques compared with physical kinematic separators arise from the possibility of using thicker targets, high beam intensities spread over larger target areas, and in providing access to nuclides emitted under large angles and low velocities. These are significant advantages not only for nuclei that are produced in hot fusion reaction with very asymmetric target-projectile combinations and reaction products with small recoil velocities but even more for multi-nucleon transfer reactions. Here chemistry experiments have an unsurpassed sensitivity. With the renewed interest in multi-nucleon transfer reactions [103, 104] and their potential to synthesize otherwise inaccessible, long-lived neutron-rich isotopes of transactinide elements chemical separation techniques, including liquid-phase chemistry, are at hand to search for and investigate such hitherto unknown nuclei.

Chemical techniques are quite feasible for the decay studies of relatively long-lived nuclei not only around a doubly magic deformed nucleus with $Z = 108$ and $N = 162$ [105] but also around a spherical superheavy elements with $Z \sim 114$. They can give a clear identification of the atomic number of relatively long-lived spontaneous fission (SF) nuclides at the end of α-decay chains of superheavy nuclei ($Z \geq 112$). The chemical identification of the newly discovered superheavy elements is highly desirable as the observed decay chains cannot be linked to known nuclides, which has been heavily criticized [106, 107]. Only in a most recent TASISpec (TASCA Small Image mode Spectroscopy) experiment, the potential of a direct identification of the atomic number of a transactinide element through “fingerprinting” in α-X-ray coincidence measurements was demonstrated [108].

References

[1] Kratz JV. Chemistry of transactinides. In: Vértes A, Nagy S, Klencsár Z, Lovas RG, Rösch F, editors. *Handbook of Nuclear Chemistry*, 2nd ed, Vol 2, Springer Science+Business Media BV; 2011, p. 925-1004.

[2] Schädel M, Shaughnessy D. *The Chemistry of Superheavy Elements*. 2nd ed. Berlin: Springer; 2014.

[3] Schädel M. Chemistry of superheavy elements. *Angew Chem Int Ed* 2006;**45**:368-401.

[4] Schädel M. Chemistry of superheavy elements. *Radiochim Acta* 2012;**100**:579-604.

[5] Türler A, Pershina V. Advances in the production and chemistry of the heaviest elements. *Chem Rev* 2013;**113**:1237-1312.

[6] Pyykkö P. Relativistic effects in structural chemistry. *Chem Rev* 1988;**88**:563-94.

[7] Pershina VG. Electronic structure and properties of the transactinides and their compounds. *Chem Rev* 1996;**96**:1977-2010.

[8] Pershina V. Electronic structure and chemistry of the heaviest elements. In: Barysz M, Ishikawa Y, editors. *Relativistic methods for chemists, Challenges and advances in computational chemistry and physics 10*, Dordrecht: Springer; 2010, p. 451-520.

[9] Kratz JV. Aqueous-phase chemistry of the transactinides. *Radiochim Acta* 2011;**99**:477-502.

[10] Kratz JV, Nagame Y. Liquid-phase chemistry of superheavy elements. In: Schädel M, Shaughnessy D, editors. *The Chemistry of Superheavy Elements*. 2nd ed. Berlin: Springer; 2014, p. 309-74.

[11] Nagame Y, Toyoshima A, Tsukada K, Asai M, Sato TK, Schädel M. Radiochemical studies of the heaviest elements at JAEA. *J Radioanal Nucl Chem* 2014;**300**:77-88.

[12] Guillaumont R, Adloff JP, Peneloux A. Kinetic and thermodynamic aspects of tracer-scale and single atom chemistry. *Radiochim Acta* 1989;**46**:169-76.

[13] Guillaumont R, Adloff JP, Peneloux A, Delamoye P. Sub-tracer behavior of radionuclides. Application to actinide chemistry. *Radiochim Acta* 1991;**54**:1-15.

[14] Borg RJ, Dienes GJ. On the validity of single atom chemistry. *J Inorg Nucl Chem* 1981;**43**:1129-33.

[15] Le Naour C, Hoffman DC, Trubert D. Fundamental and experimental aspects of single atom-at-a-time chemistry. In: Schädel M, Shaughnessy D, editors. *The Chemistry of Superheavy Elements*. 2nd ed. Berlin: Springer; 2014, p. 241-60.

[16] Seaborg GT. The chemical and radioactive properties of the heavy elements. *Chem Eng News* 1945;**23**:2190-3.

[17] Ghiorso A, Nurmia M, Eskola K, Eskola P. ^{261}Rf; New isotope of element 104. *Phys Lett B* 1970;**32**:95-8.

[18] Silva RJ, Harris J, Nurmia M, Eskola K, Ghiorso A. Chemical separation of rutherfordium. *Inorg Nucl Chem Lett* 1970; **6**:871-7.

[19] Hulet EK, Lougheed RW, Wild JF, Landrum JH, Nitschke JM, Ghiorso A. Chloride complexation of element 104. *J Inorg Nucl Chem* 1980;**42**:79-82.

[20] Haba H, Tsukada K, Asai M, Goto S, Toyoshima A, Nishinaka I et al. Anion-exchange behavior of Rf in HCl and HNO_3 solutions. *J Nucl Radiochem Sci* 2002;**3**:143-6.

[21] Günther R, Paulus W, Kratz JV, Seibert A, Thörle P, Zauner S et al. Chromatographic study of rutherfordium (element 104) in the system HCl/Tributylphosphate (TBP). *Radiochim Acta* 1998;**80**;121-8.

[22] Haba H, Tsukada K, Asai M, Toyoshima A, Ishii Y, Toume H et al. Extraction behavior of rutherfordium into tributylphosphate from hydrochloric acid. *Radiochim Acta* 2007;**95**:1-6.

[23] Toyoshima A, Kasamatsu Y, Tsukada K, Asai M, Ishii Y, Toume H et al. Extraction chromatographic behavior of Rf, Zr, and Hf in HCl solution with styrene-divinylbenzene copolymer resin modified by TOPO (trioctylphosphine oxide). *J Nucl Radioche.m Sci* 2010;**11**:7-11.

[24] Strub E, Kratz JV, Kronenberg A, Nähler A, Thörle P, Zauner S et al. Fluoride complexation of rutherfordium (Rf, element 104). *Radiochim. Acta* 2000;**88**:265-71.

[25] Ishii Y, Toyoshima A, Tsukada K, Asai M, Toume H, Nishinka I et al. Fluoride complexation of element 104, rutherfordium (Rf), investigated by cation-exchange chromatography. *Chem Lett* 2007;**37**:288-9.

[26] Ishii Y, Toyoshima A, Tsukada K, Asai M, Li ZJ, Nagame Y et al. Fluorido complex formation of element 104, rutherfordium (Rf). *Bull Chem Soc Jpn* 2011;**84**:903-11.

[27] Haba H, Tsukada K, Asai M, Toyoshima A, Akiyama K, Nishinaka I et al. Fluoride complexation of element 104, rutherfordium. *J Am Chem Soc* 2004;**126**:5219-24.

[28] Toyoshima A, Haba H, Tsukada K, Asai M, Akiyama K, Nishinaka I et al. Elution curve of rutherfordium (Rf) in anion-exchange chromatography with hydrofluoric acid solution. *J Nucl Radiochem Sci* 2004;**5**:45-8.

[29] Toyoshima A, Haba H, Tsukada K, Asai M, Akiyama K, Goto S et al. Hexafluoro complex of rutherfordium in mixed HF/HNO_3 solutions. *Radiochim Acta* 2008;**96**:125-34.

[30] Li ZJ, Toyoshima A, Asai M, Tsukada K, Sato TK, Sato N et al. Sulfate complexation of element 104, Rf, in H_2SO_4/HNO_3 mixed solution. *Radiochim Acta* 2012;**100**:157-64.

[31] Schädel M, Brüchle W, Schimpf E, Zimmermann HP, Gober MK, Kratz JV et al. Chemical properties of element 105 in aqueous solution: Cation exchange separation with α-hydroxyisobutyric acid. *Radiochim Acta* 1992;**57**:85-92.

[32] Kratz JV, Zimmermann HP, Scherer UW, Schädel M, Brüchle W, Gregorich KE, et al. Chemical properties of element 105 in aqueous solution: Halide complex formation and anion exchange into triisooctyl amine. *Radiochim Acta* 1989;**48**:121-33.

[33] Zimmermann HP, Gober MK, Kratz JV, Schädel M, Brüchle W, Schimpf E et al. Chemical properties of element 105 in aqueous solution: Back extraction from triisooctyl amine into 0.5 M HCl. *Radiochim Acta* 1993;**60**:11-6.

[34] Gober MK, Kratz JV, Zimmermann HP, Schädel M, Brüchle W, Schimpf E et al. Chemical properties of element 105 in aqueous solution: Extraction into diisobutylcarbinol. *Radiochim Acta* 1992;**57**:77-84.

[35] Paulus W, Kratz JV, Strub E, Zauner S, Brüchle W, Pershina V et al. Chemical properties of element 105 in aqueous solution: Extraction of the fluoride-, chloride-, and bromide complexes of the group-5 elements into anapliphatic amine. *Radiochim Acta* 1999;**84**:69-77.

[36] Tsukada K, Haba H, Asai M, Toyoshima A, Akiyama K et al. Adsorption of Db and its homologues Nb and Ta, and the pseudo-homologue Pa on anion-exchange resin in HF solution. *Radiochim Acta* 2009;**97**:83-9.

[37] Kasamatsu Y, Toyoshima A, Asai M, Tsukada K, Li ZJ, Ishii Y et al. Anionic fluoro complex of element 105, Db. *Chem Lett* 2009;**38**:1084-5.

[38] Schädel M, Brüchle W, Dressler R, Eichler B, Gäggeler HW, Günther R et al. Chemical properties of element 106 (seaborgium). *Nature* 1997;**388:**55-7.

[39] Schädel M, Brüchle W, Schausten B, Schimpf E, Jäger E, Wirth G etal. First aqueous chemistry with seaborgium (element 106). *Radiochim Acta* 1997;**77**:149-59.

[40] Schädel M, Brüchle W, Jäger E, Schausten B, Wirth G, Paulus W, et al. Aqueous chemistry of seaborgium (*Z* = 106). *Radiochim Acta* 1998;**83**:163-5.

[41] Schädel M, Brüchle W, Jäger E, Schimpf E, Kratz JV, Scherer UW, Zimmermann HP. ARCA II - A new apparatus for fast, repetitive HPLC separations. *Radiochim Acta* 1989;**48**:171-6.

[42] Nagame Y, Tsukada K, Asai M, Toyoshima A, Akiyama K, Ishii Y et al. Chemical studies on rutherfordium (Rf) at JAEA. *Radiochim Acta* 2005;**93**:519-26.

[43] Türler A, Gregorich KE. Experimental techniques. In: Schädel M, Shaughnessy D, editors. *The Chemistry of Superheavy Elements*. 2nd ed. Berlin: Springer; 2014, p. 261-308.

[44] Plaisance PM, Guillaumont R. Fluoro- et chlorofluoro-complexes de protactiniumpentavalent. *Radiochim Acta* 1969;**12**:32-7.

[45] Kim JI, Lagally H, Born H-J. Ion exchange in aqueous and in aqueous-organic solvents: Part I. Anion-exchange behaviour of Zr, Nb, Ta and Pa in aqueous HCl-HF and in HCl-HF-organic solvent. *Anal. Chim. Acta* 1973;**64**:29-43.

[46] Korkisch J. *Handbook of Ion Exchange Resins: Their Application to Inorganic and Analytical Chemistry*, Boca Raton, FL, CRC Press; 1989.

[47] Pearson RG. Hard and soft acids bases. *J Am Chem Soc* 1963;**85**:3533- 9.

[48] Pearson RG. Hard and soft acids and bases, HSAB, part I. *J Chem Edu* 1968;**45**:581-7.

[49] Pearson RG. Hard and soft acids and bases, HSAB, part II. *J Chem Edu* 1968;**45**:643-8.

[50] Pershina V, Trubert D, Le Naour C, Kratz JV. Theoretical predictions of hydrolysis and complex formation of group-4 elements Zr, Hf, and Rf in HF and HCl solutions. *Radiochim Acta* 2002;**90**:869-77.

[51] Shannon RD. Revised effective ionic radii and systematic studies of interatomic distances in halides and chalcogenides. *Acta Cryst* 1976;**A32**:751-67.

[52] Pershina V. Theoretical chemistry of the heaviest elements. In: Schädel M, Shaughnessy D, editors. *The Chemistry of Superheavy Elements*. 2nd ed. Berlin: Springer; 2013, p. 135-239.

[53] Ryabchikov DI, Marov IN, Ermakov AN, Belyaeva VK. Stability of some inorganic and organic complex compounds of zirconium and hafnium. *J Inorg Nucl Chem* 1964;**26**:965-80.

[54] Pershina V, Polakova D, Omtvedt JP. Theoretical prediction of complex formation of group-4 elements Zr, Hf, and Rf in H_2SO_4 solutions. *Radiochim Acta* 2006;**94**:407-14.

[55] Haba H, Akiyama K, Tsukada K, Asai M, Toyoshima A, Yaita T et al. Chloride complexation of Zr and Hf in HCl investigated by extended x-ray absorption fine structure spectroscopy: Toward characterization of chloride complexation of element 104, rutherfordium (Rf). *Bull Chem Soc Jpn* 2006;**82**:698-703.

[56] Pai SA, Subramanian MS. Synergetic extractions of uranyl ions with 1-phenyl-3-methly-benzoylpyrazolone-5 (HPMBP) and diphenyl sulfoxide (DPSO), tri-n-butyl phosphate (TBP) or tri-n-octylphosphine oxide (TOPO). *J Radioanal Nucl Chem* 1985;**89**:423-433.

[57] Rizvi GH. Extraction of actinides with tropolone I. Synergistic extraction of uranium(VI) with tropolone and some neutral donors. *J Radioanal Nucl Chem* 1993;**170**:479-487.

[58] Omtvedt JP, Alstad J, Breivik H, Dyve JE, Eberhardt K, Folden III CM et al. SISAK liquid-liquid extraction experiments with preseparated ^{257}Rf. *J Nucl Radiochem Sci* 2002;**3**:121-4.

[59] Stavsetra L, Gregorich KE, Alstad J, Breivik H, Eberhardt K, Folden III CM et al. Liquid-scintillation detection of preseparated ^{257}Rf with the SISAK-system. *Nucl Instr Meth Phys Res A* 2005;**543**:509-16.

[60] Gregorich KE, Henderson RA, Lee DM, Nurmia MJ, Chasteler RM, Hall HL et al. Aqueous chemistry of element 105. *Radiochim Acta* 1988;**43**:223-31.

[61] Pershina V, Fricke B, Kratz JV, Ionova GV. The electronic structure of anionic halide complexes of element 105 in aqueous solutions and their extraction by aliphatic amines. *Radiochim Acta* 1994;**64**:37-48.

[62] Pershina V. Solution chemistry of element 105 Part I: Hydrolysis of group 5 cations: Nb, Ta, Ha and Pa. *Radiochim Acta* 1998;**80**:65-73.

[63] Pershina V. Solution chemistry of element 105 Part II: Hydrolysis and complex formation of Nb, Ta, Ha and Pa in HCl solutions. Radiochim Acta 1998;**80**:75-84.

[64] Nagame Y, Asai M, Haba H, Goto S, Tsukada K, Nishinaka I et al. Production cross sections of ^{261}Rf and ^{262}Db in bombardments of ^{248}Cm with ^{18}O and ^{19}F ions. *J Nucl Radiochem Sci* 2002;**3**:85-8.

[65] Kasamatsu Y, Toyoshima A, Haba H, Toume H, Tsukada L, Akiyama K et al. Adsorption of Nb, Ta and Pa on anion-exchanger in HF and HF/HNO_3 solutions: Model experiments for the chemical study of Db. *J Radioanal Nucl Chem* 2009;**279**:371-6.

[66] Myasoedov BF, Kirby HW, Tananaev IG. Protoactinium. In: Morss LR, Edelstein NM, Fuger J, editors. *The Chemistry of the Actinide and Transactinide Elements*, 3rd ed, Vol 1, Dordrecht: Springer; 2006, p. 161-252.

[67] Di Giandomenico MV, Le Naour C, Simoni E, Guillaumont D, Moisy Ph, Hennig C et al. Structure of early actinides (V) in acidic solutions. *Radiochim Acta* 2009;**97**:347-53.

[68] Dmitriev SN, Oganessyan Yu Ts, Utyonkov VK, Shishkin SV, Yeremin AV, Lobanov YV et al. Chemical identification of dubnium as a decay product of element 115 produced in the reaction ^{48}Ca + ^{243}Am. *Mendeleev Commun.* 2005;**15**:1-4.

[69] Schumann D, Bruchertseifer H, Eichler R, Eichler B, Gäggeler HW, Dmitriev SN et al. Chemical procedure applied for the identification of Rf/Db produced in the ^{48}Ca + ^{243}Am reaction. *Radiochim Acta* 2005;**93**:727-32.

[70] Oganessian Yu Ts, Utyonkov VK., Dmitriev SN, Lobanov Yu V, Itkis MG, Polyakov AN et al. Synthesis of elements 115 and 113 in the reaction ^{243}Am + ^{48}Ca. *Phys Rev C* 2005;**72**:034611(16).

[71] Oganessian Yu Ts, Utyonkov VK, Lobanov Yu V, Abdullin F Sh, Polyakov AN, Shirokovsky IV et al. Experiments on the sysnthesis of element 115 in the reaction ^{243}Am(^{48}Ca, *xn*)$^{291-x}$115. *Phys Rev C* 2004;**69**:021601(5).

[72] Lazarev Yu A, Lobanov Yu V, Oganessian Yu Ts, Utyonkov VK, Abdullin F Sh, Buklanov GV et al. Discovery of enhanced nuclear stability near the deformed shells N = 162 and Z = 108. *Phys Rev Lett* 1994;**73**:624-7.

[73] Türler A, Brüchle W, Dressler R, Eichler B, Gäggeler HW, Gregorich KE et al. Decay properties of ^{265}Sg (Z = 106) and ^{266}Sg (Z = 106). *Phys Rev C* 1998;**57**:1648-55.

[74] Düllmann Ch E, Türler A. ^{248}Cm(^{22}Ne, *xn*)$^{270-x}$Sg reaction and the decay properties of ^{265}Sg reexamined. *Phys Rev C* 2008; **77:**064320(10).

[75] Haba H, Kaji D, Kikunaga H, Kudou Y, Morimoto K, Morita K et al. Production of ^{265}Sg in the ^{248}Cm(^{22}Ne, 5*n*)^{265}Sg reaction and decay properties of two isomeric states in ^{265}Sg. *Phys Rev C* 2012;**85**:024611(11).

[76] Toyoshima A, Kasamatsu Y, Kitatasuji Y, Tsukada K, Haba H, Shinohara A et al. Development of an electrochemistry apparatus for the heaviest elements. *Radiochim Acta* 2008;**96**:323-6.

[77] Toyoshima A, Kasamatsu Y, Tsukada K, Asai M, Kitatsuji Y, Ishii Y et al. Oxidation of element 102, nobelium, with flow electrolytic column chromatography on an atom-at-a-time scale. *J Am Chem Soc* 2009;**131**:9180-1.

[78] Toyoshima A, Li Zijie, Asai M, Sato N, Sato TK, Kikuchi T et al. Measurement of the Md^{3+}/Md^{2+} reduction potential studied with flow electrolytic chromatography. *Inorg Chem* 2013;**52**:12311-3.

[79] Kratz JV, Pershina V. Experimental and theoretical study of the chemistry of the heaviest elements. In: Hess BA, editor, *Relativistic effects in heavy-element chemistry and physics*, West Sussex, England, John Wiley & Sons; 2003, Chapter 6, p. 219-44.

[80] Pershina V. Predictions of redox potentials of Sg in acid solutions as a function of pH. *Radiochim Acta* 2013;**101**:749-52

[81] Toyoshima A, Ooe K, Miyashita S, Asai M, Attallan MF, Goto N et al. Chemical studies of Mo and W in preparation of a seaborgium (Sg) reduction experiment using MDG, FEC, and SISAK. *J Radioanal Nucl Chem* 2015;**303**:1169-72.

[82] Omtvedt JP, Alstad J, Bjørnstad T, Düllmann ChE, Gregorich KE, Hoffman DC et al. Chemical properties of the transactinide elements studied in liquid phase with SISAK. *Eur Phys J A* 2007;**45**:91-7.

[83] Ooe K, Attallah MF, Asai M, Goto N, Gupta NS, Haba H et al. Development of a new continuous dissolution apparatus with a hydrophobic membrane for superheavy element chemistry. *J Radioanal Nucl Chem* 2015;**303**:1317-20.

[84] Haba H, Kaji D, Komori Y, Kudou Y, Morimoto K, Morita K, et al. RIKEN Gas-filled recoil ion separator (GARIS) as a promising interface for superheavy element chemistry -Production of element 104, ^{261}Rf, using the GARIS/gas-jet system-. *Chem Lett* 2009;**38**:426-7.

[85] Strub E. Doctoral dissertation 2000, University of Mainz, Germany.

[86] Eichler B, Kratz JV. Electrochemical deposition of carrier-free radionuclides. *Radiochim Acta* 2000;**88**:475-82.

[87] Hummrich H, Banik NL, Breckheimer M, Brüchle W, Buda R, Feist F et al. Electrodeposition methods in superheavy element chemistry. *Radiochim Acta* 2008;**96**:73-83.

[88] Liang XH, Tsukada K, Toyoshima A, Li ZJ, Asai M, Sato TK et al. Adsorption behavior of ^{181}W and ^{93m}Mo as lighter homologues of seaborgium (Sg) in HF/HNO_3 on anion-exchange resin. *J Radioanal Nucl Chem* 2012;**292**:917-22.

[89] Hild D, Eberhardt K, Even J, Kratz JV, Wiehl N, Löb P et al. MicroSISAK: continuous liquid-liquid extractions of radionuclides at ≥ 0.2 mL/min. *Radiochim Acta* 2013;**101**:681-9.

[90] Oganessian YuTs. Heaviest nuclei from ^{48}Ca-induced reactions. *J Phys G: Nucl Part Phys* 2007;**34**:R165-242.

[91] Kratz JV, Nähler A, Rieth U, Kronenberg A, Kuczewski B, Strub E et al. An EC-branch in the decay of 27-s ^{263}Db: Evidence for the isotope ^{263}Rf. *Radiochim Acta* 2003;**91**:59-62.

[92] Kratz JV, Gober MK, Zimmermann HP, Schädel M, Brüchle W, Schimpf E et al. New nuclide ^{263}Hs. *Phys Rev C* 1992;**45**:1064-9.

[93] Even J, Yakushev A, Düllmann Ch E, Haba H, Asai M, Sato TK et al. Synthesis and detection of a seaborgium carbonyl complex. *Science* 2014;**345**:1491-3.

[94] Eichler R, Brüchle W, Dressler R, Düllmann Ch E, Eichler B, Gäggeler HW et al. Chemical characterization of bohrium (element 107). *Nature* 2000;**407**:63-5.

[95] Düllmann Ch E, Brüchle W, Dressler R, Eberhardt K, Eichler B, Eichler R et al. Chemical investigation of hassium (element 108). *Nature* 2002;**418**:859-62.

[96] Türler A, Düllmann Ch E, Gäggeler HW, Kirbach UW, Yakushev AB, Schädel M et al. On the decay properties of ^{269}Hs and indications for the new nuclide ^{270}Hs. *Eur Phys J A* 2003;**17**:505-8.

[97] Dvorak J, Brüchle W, Chelnokov M, Düllmann Ch E, Dvorakova Z, Eberhardt K et al. Doubly magic nucleus $^{270}_{108}Hs_{162}$. *Phys Rev Lett* 2006;**97**:242501(4).

[98] Dvorak J, Brüchle W, Chelnokov M, Düllmann Ch E, Dvorakova Z, Eberhardt K et al. Observation of the 3*n* evaporation channel in the complete hot-fusion reaction ^{26}Mg + ^{248}Cm leading to the new superheavy nuclide ^{271}Hs. *Phys Rev Lett* 2008;**100**:132503(4).

[99] Eichler R, Aksenov NV, Belozerov AV, Bozhikov GA, Chepigin VI, Dmitriev SN et al. Chemical characterization of element 112. *Nature* 2007;**447**:72-5.

[100] Eichler R, Aksenov NV, Belozerov AV, Bozhikov GA, Chepigin VI, Dmitriev SN et al. Thermochemical and physical properties of element 112. *Angew Chem Int Ed* 2008;**47**:3262-6.

[101] Dmitriev SN, Aksenov NV, Albin YV, Bozhikov GA, Chelnokov ML, Chepygin VI et al. Pioneering experiments on the chemical properties of element 113. *Mendeleev Commun* 2014;**24**:253-6.

[102] Yakushev A, Gates JM, Türler A, Schädel M, Düllmann Ch E, Ackermann D et al. Superheavy element flerovium (element 114) is a volatile metal. *Inorg Chem* 2014;**53**:1624-9.

[103] Zagrebaev VI, Oganessian YuTs, Itkis MG, Greiner W. Superheavy nuclei and quasi-atoms produced in collisions of transuranium ions. *Phys Rev C* 2006;**73**,031602(R).

[104] Kratz JV, Schädel M, Gäggeler HW. Reexamining the heavy-ion reactions ^{238}U+^{238}U and ^{238}U+^{248}Cm and actinide production close to the barrier. *Phys Rev C* 2013;**88**:054615(19).

[105] Sobiczewski A, Pomorski K. Description of structure and properties of superheavy nuclei. *Prog Part Nucl Phys* 2007;**58**:292-349.

[106] Armbruster P. On the quest of production of superheavy nuclei in reactions of ^{48}Ca with the heaviest actinide targets. *Eur Phys J A* 2000;**7**,23-33.

[107] Armbruster P. On the production of superheavy elements. *Annu Rev Nucl Part Sci* 2000;**50**:411-79.

[108] Rudolph D, Forsberg U, Golubev P, Sarmiento LG, Yakushev A, Andersson L-L et al. Spectroscopy of element 115 decay chains. *Phys Rev Lett* 2013;**111**:112502(5).